Received: 16 September 2024 | Revised: 26 January 2025 | Accepted: 5 February 2025

DOI: 10.1096/fj.202402212RR

RESEARCH ARTICLE

The FASEB Journal

Insights into the single-cell transcriptome characteristics of porcine endometrium with embryo loss

Tingting Chu[1] | **Yadan Jin**[2] | **Guofang Wu**[3] | **Jinyi Liu**[1] | **Shiduo Sun**[1] | **Yuxuan Song**[1] | **Guoliang Zhang**[2]

[1]College of Animal Science and Technology, Northwest A&F University, Yangling, Shaanxi, P.R. China

[2]College of Animal Science and Technology, Qingdao Agricultural University, Qingdao, Shandong, P.R. China

[3]College of Animal Husbandry and Veterinary Science, Qinghai University, Xining, Qinghai, P.R. China

Correspondence
Guoliang Zhang, College of Animal Science and Technology, Qingdao Agricultural University, Qingdao, Shandong 266109, P.R. China.
Email: 201901022@qau.edu.cn

Yuxuan Song, College of Animal Science and Technology, Northwest A&F University, Yangling, Shaanxi 712100, P.R. China.
Email: yuxuan_song2016@163.com

Funding information
MOST | NSFC | National Natural Science Foundation of China-Shandong Joint Fund, Grant/Award Number: 31902158; Key Technology Research and Development Program of Shandong Province, Grant/Award Number: 2021LZGC001; Modern Agricultural Technology Industry System of Shandong province, Grant/Award Number: SD-AIT-08-16; Natural Science Foundation of Shandong Province, Grant/Award Number: ZR2020QC099; Natural Science Foundation of Qingdao Municipality (Qingdao Natural Science Foundation), Grant/Award Number: 24-4-4-zrjj-144-jch; Shaanxi Pig Industry Technology System Breeding and Promotion Integration Project, Grant/Award Number: K3031222128; Research Foundation for Advanced Talents of Qingdao Agricultural University, Grant/Award Number: 665/1119013

Abstract

Reproductive disorders are a concern in the pig industry. Successful gestation processes are closely related to a suitable endometrial microenvironment, and the physiological mechanisms leading to failed pregnancy during the peri-implantation period remain unclear. We constructed single-cell transcriptome profiles of peri-implantation embryo loss and successful gestation endometrial tissues and identified 22 cell subpopulations, with epithelial and stromal cells being the predominant endometrial cell types. The two tissues showed marked differences in cell type composition, especially among epithelial cell subpopulations. We also observed functional differences between epithelial and stromal cells in tissues from embryonic loss and successful gestation, as well as the expression levels and differentiation trajectories of genes associated with embryo attachment and endometrial receptivity in epithelial and stromal cells. The results of cell communication interactions analysis showed that ciliated cells were more active in endometrial tissue with embryo loss, and there were differences in the types of endometrial cells with major roles in embryo loss and embryo implantation successful tissues for bone morphogenic protein, insulin-like growth factor, and transforming growth factor-β signaling networks associated with embryo implantation. In addition, we compared the functional differences in immune cells between the two tissue types and the expression levels of genes related to the inflammatory microenvironment. Overall, the present study revealed the molecular features of endometrial cell transcription in embryo-lost endometrial tissues, providing deeper insights into the endometrial microenvironment of reproductive disorders, which may inform the etiological, diagnostic, and therapeutic studies of reproductive disorders.

KEYWORDS
ciliated cells, embryo implantation, endometrium, transcriptome

1 | INTRODUCTION

Reproductive traits are among the most important economic traits in the swine industry, and the annual litter size of a sow is determined by the ability to maintain viable embryos throughout gestation.[1,2] Successful embryo implantation is also strongly associated with successful pregnancy and litter size.[3,4] Approximately 75% of pregnancy losses are due to implantation failure.[5] Thirty percent of porcine embryos are lost between days 12 and 30 of gestation,[6] and the mortality rate of embryos in the case of embryo transfer is about 70%.[7] Successful pregnancy is synergistically regulated by multiple molecular mechanisms, the process of embryo implantation requires concerted interaction between the blastocyst and the endometrium,[8] morphologic and functional changes in the endometrium are key determinants of uterine receptivity to the embryo, and during early gestation, hormones, growth factors, and transit proteins in the uterine cavity promote the growth and development of the embryo.[9] Conceptus secretory factors activate endometrial genes to stimulate uterine modulation of immune responses.[10] Endometrial receptivity disorders, defects in gene function, and defects in maternal-fetal crosstalk lead to failure of embryo implantation and even recurrent pregnancy failure and infertility.[4,11,12] However, the porcine endometrial characteristics of embryo loss have not yet been fully elucidated, and a comprehensive understanding of the molecular characterization of the endometrium in reproductive disorders is important for improving reproductive performance.

The endometrium is a complex tissue composed of multiple cell types, mainly epithelial cells, stromal cells, and various types of immune cells.[13] During the early stages of embryo implantation, the trophoblast ectoderm of the blastocyst can attach to endometrial epithelial cells and then proceed to invade the endometrial stroma and vasculature.[14] Enrichment of natural killer (NK) cells occurs at the conceptus attachment sites, and the maternal immune environment undergoes dynamic changes to achieve a homeostatic immune state regulated by hormonal cytokines and inflammatory mediators secreted by the embryo during implantation, leading to the establishment of a pro-inflammatory environment during implantation.[15] It has been suggested that disturbances in immune-promoted endometrial angiogenesis are some of the main causes of subsequent fetal abortions and reduced litter sizes in pigs.[16] Recent tissue-wide transcriptomics-based analysis reveals molecular-level differences in endometrial dysfunctional tissues with failed embryonic attachment.[17] However, owing to cellular heterogeneity and the unique role of different cell types in embryo implantation, the transcriptional profiles of different cell types in endometrial tissues with embryo loss remain to be further clarified.

Single-cell RNA sequencing can dissect cellular heterogeneity and analyze molecular alterations at the cellular level, capturing key cell populations of change and their transcriptional signatures, providing greater insight into cellular processes important in tissue development and disease progression.[18] In this study, we developed single-cell mapping of embryo loss and attachment success in the endometrium, captured key cell populations with altered endometrial organization in embryo loss, and analyzed their molecular signatures.

2 | MATERIALS AND METHODS

2.1 | Sample collection

All experimental animals were 3 years old with a similar genetic background. We selected a Yorkshire sow with an abortion experience on the 26th of gestation, after three consecutive artificial insemination matings, and subsequently there were no returns of sows to estrous phenomenon. After 30 days, no developing fetus was seen in the sample when we collected the endometrium tissues, which represented the sample of embryo loss (EL). Another Yorkshire sow with successful artificial insemination was selected and gestated for 30 days; the 30-day embryos were obviously observed when endometrial samples were collected, which represented the sample of successful embryo implantation (EIS). We defined the day of artificial insemination as day 0 of pregnancy, and endometrial samples were collected from each uterine horn; animals requiring slaughter were humanely euthanized as necessary to relieve suffering, all experimental procedures were approved by the Animal Care and Use Committee of Qingdao Agricultural University (DEC, 2024-0079), Qingdao, China.

2.2 | Single-cell dissociation

About 200 mg of endometrial tissue was clipped, washed twice with precooled phosphate-buffered saline (PBS) solution, placed in tissue protection solution (BioYou, 21903-10), and transferred to the laboratory on ice for follow-up treatment. After adding enzyme digestion solution (2 mg/mL collagenase II, 1 mg/mL dispersed protease, 30 μg/mL DNase I, 2.5 mM CaCl2, containing FBS 2% dissolved in basal medium), the samples were shaken in a 37°C water bath shaker at 100 rpm/min for 20 min. The enzyme-digested suspension was filtered through a 30 μm cell filter and added to 15 mL PBS, centrifuged at

500 *g* for 5 min at 4°C. The supernatant was removed and the pellet resuspended with 1 mL of 0.04% BSA, added into 3 mL of 1X RBC to lyse erythrocytes, and left at room temperature for 5 min (the time can be adjusted according to the actual situation of erythrocyte lysis). The suspension was then washed twice with PBS and centrifuged at 4°C, 300 *g* for 5 min. The supernatant was removed and the pellet resuspended in 500 μL of 0.04% BSA. Cell parameters were then tested with a cell counter (CountessTM II FL Automated Cell Counter, Thermo Fisher Scientific, Waltham, MA, USA).

2.3 | Single-cell RNA-seq library preparation and sequencing

The scRNA-Seq libraries and RNA sequencing were performed by Gene Denovo Biotechnology Co., LTD (Guangzhou, China). A Chromium NextGEM Chip G Single Cell Kit (PN- 1000120; 10X Genomics, Pleasanton, CA, USA) was used to construct scRNA-Seq libraries. In brief, single cell suspensions at a concentration of 1000 cells/μL were loaded onto the chip in a 10X Genomics Chromium Controller (10X Genomics) to generate single cell gel bead emulsions (GEMs), GEMS were subjected to PCR followed by GEMS-RT bead purification and cDNA amplification. The purified cDNA product was fragmented, end-repaired, A-tailed, and ligated with adaptors, and amplification by PCR. Finally, the DNA 1000 assay Kit (5067-1505, Agilent Technologies, Santa Clara, CA, USA) was used for library QC, and the ABI StepOnePlus Real-Time PCR System (Life Technologies, Carlsbad, CA, USA) was used for quantification and pooling according to the Novaseq 6000 PE150 mode for online sequencing.

2.4 | Single-cell RNA statistical analysis

Data quality statistics were performed on raw data using Cell Ranger v3.1.0. First, the Read2 cDNA sequence fragments were aligned to the reference genome (GCF_000003025.6_Sscrofa11.1_v3) by STAR (Spliced Transcripts Alignment to a Reference), followed by filtering and correcting barcodes and UMIs, filtering out single oligo strands, UMIs with N and mass values less than 10 bases, and validated reads of barcodes and UMIs were further used for UMI counting. Based on the EmptyDrops[19] method to determine valid barcodes, the UMI corresponding to each gene ID of each barcode was de-emphasized, and the number of unique UMIs was calculated as the expression of the gene in the cell. Single-cell transcriptome data were analyzed using the R package Seurat[20] for further quality control, analysis, and data exploration. Finally, the UMAP package is used to map the high-dimensional data to two-dimensional space for visual display and analysis, and the default Wilcoxon rank-sum test was used to calculate the marker genes of each cell cluster under the following criteria with log FC threshold = 0.25 and min.pct = 0.25, differentially expressed genes (DEGs) among cell clusters in pseudotime with *q*val <.01, and DEGs between two samples with |log2FC| = 0.5 and *p*-value <.05 were used.

2.5 | Functional enrichment analysis

Functional annotation of highly expressed differential marker genes in cell populations was performed using the Kyoto Encyclopedia of Genes and Genomes (KEGG) (https://www.kegg.jp/) and Gene Ontology (GO) databases (http://www.geneontology.org/).

2.6 | Cell communication analysis

Cell Phone DB V5 software was used to predict ligand-receptor interactions between two cell states and potential communication relationships between cell pairs by constructing networks of interactions between cell types.

2.7 | Pseudotime analysis

Monocle2 (http://cole-trapnell-lab.github.io/monocle-release) was used to perform single-cell trajectory analysis. Briefly, the cellular gene expression matrix was entered into Monocle2 and Monocle2 was utilized to downscale the data to a two-dimensional plane. The screening criteria for differential genes based on differentiation status and proposed temporal changes were corrected with a *p*-value <.1.

2.8 | RNA extraction, reverse transcription, real-time fluorescence quantification-PCR

According to the manufacturer's protocol, total RNA was extracted from the endometrial tissues using the SevenFast® Total RNA Extraction Kit (SM130-02, Seven Biotech, Beijing, China). A microplate spectrophotometer (Epoch, BioTek Instruments Inc., USA) was used to detect RNA concentration and quality, the range of OD_{260}/OD_{280} is 1.8–2.0. The RNA was synthesized to cDNA by using the Takara One Step Reverse Transcription Kit (RR092A, Takara Bio Inc. Co. Ltd., Japan) as directed

by the manufacture. The primers information used in qRT-PCR were designed by Oligo 7 software, relative gene expression was quantified by real-time fluorescence quantitative PCR by using the 2×FastHS SYBR QPCR Mixture (AM2101, Allmeek, China). The detailed conditions for qRT-PCR were as follows: 95°C for 30 s, followed by 40 cycles of 95°C for 10 s, and 60°C for 30 s. Data were analyzed using the $2^{-\Delta\Delta Ct}$ method with GAPDH as a reference. The detailed qRT-PCR primers information is listed in Table S17.

2.9 | Hematoxylin–eosin (HE) staining and immunohistochemistry analysis

Fresh tissue was fixed with 4% paraformaldehyde, dehydrated with alcohol in turn, embedded in paraffin wax, and sliced, then stained with hematoxylin and eosin. The deparaffinized tissue sections are antigenically repaired, and primary antibodies COL1A1 (Huabio, ET1609-68) and ACTA2 (Proteintech, 67735-1-Ig) are added. Sections were incubated at 4°C overnight. After washing out the primary antibodies, after tissue sections were closed with 5% BSA (BioFROXX, EZ2811C238) at room temperature for 1 h, the secondary antibodies (Fuzhou Maixin Immunohistochemistry Kit, KIT9730), and DAB chromogen (Fuzhou Maixin, DAB-1031) were added for visualization. Subsequently, nuclear staining was performed using hematoxylin. Next, the tissue sections were dehydrated and sealed. The image was captured using a slide scan system via SlideViewer version 1.5.5.2 software.

2.10 | Statistical analysis

The data analysis was performed using independent samples *t*-tests by SPSS 23.0 software (IBM Corp.), data visualization was by using GraphPad Prism 5 (GraphPad InStat Software). Data are presented as the mean ± SEM. A *p*-value <.05 was considered statistically significant, and $p < .01$ was considered extremely significant.

3 | RESULTS

3.1 | Identification of porcine endometrial cell type

To investigate the cellular transcription features of failed pregnancy endometrial tissue, scRNA-seq was performed to characterize the differential endometrial transcriptional landscape in EL and EIS tissue (Figure 1A,B and Table S1). We obtained a total of 10687 and 8661 endometrial single-cell transcriptomes from EL and EIS tissue respectively (Figure S1A), and further identified major cell types based on maker genes, epithelial cells (*KRT8, KRT18, MSX1*),[6,21] stromal cells (*DCN, PGR*) and lymphocytes (*PTPRC*),[6] monocyte/macrophage (*TYROBP*),[22] and endothelial cells (*PECAM1*, *CLDN5*)[21] were identified from previous studies, fibroblasts (*ACTA2*), ciliated cells (*FOXJ1*), and NK cells (*CD8A, CD3D, NKG7*) were identified from CellMaker2.0 (Figure 1D–J and Table S2). Concurrently, we identified 11 epithelial cell subpopulations and observed epithelial cells 2 and 4 as the main epithelial cell populations in EIS tissue, while epithelial cells 1 and 3 were the main epithelial cell populations in EL tissue (Figure 1C). KEGG pathway enrichment analysis was performed to compare the functional differences of these epithelial cell subpopulations. The lysine degradation pathway was mainly enriched in epithelial cell 1, and epithelial cell 3 was related to thermogenesis, oxidative phosphorylation, and reactive oxygen species signaling pathways. Epithelial cells 2 and 4 had similar functional pathways, and the ribosome pathway was significantly enriched in epithelial cell 4 (Figure S1B–E). Moreover, the number of ciliated epithelial cells was higher in EL tissues (Figure 1C).

In addition, the DEGs analysis between two groups based on clusters showed that there are 320 genes that were up-regulated in EL tissue, 174 genes that were down-regulated, and qRT-PCR results were consistent with transcriptional sequencing results (Figure S2A). HE staining analysis showed that a greater number of glands in EL endometrial tissue (Figure S2B), IHC analysis showed COL1A1 protein was highly expressed in endometrial tissue, we similarly noted that ACTA2 was expressed in EL and EIS tissues, and the EIS tissue showed a higher expressional level (Figure S2C).

Overall, we established a single-cell transcriptome profile of endometrial cells from EL and EIS tissues, where epithelial and stromal cells were the major cell populations in endometrial tissues, and EL tissues presented obvious differences in microenvironmental cell components.

3.2 | Transcriptional atlas of endometrial cells in EL tissues

To systematically elaborate the complex cellular mechanism of embryo loss, we next isolated and identified fourteen cell types in the EL endometrial atlas, mainly including epithelial cells, stromal cells, and immunity cells (Figure 2A and Table S3). Figure 2B shows the top expression level of marker genes in each cell type populations (Table S4). GO enrichment analysis showed

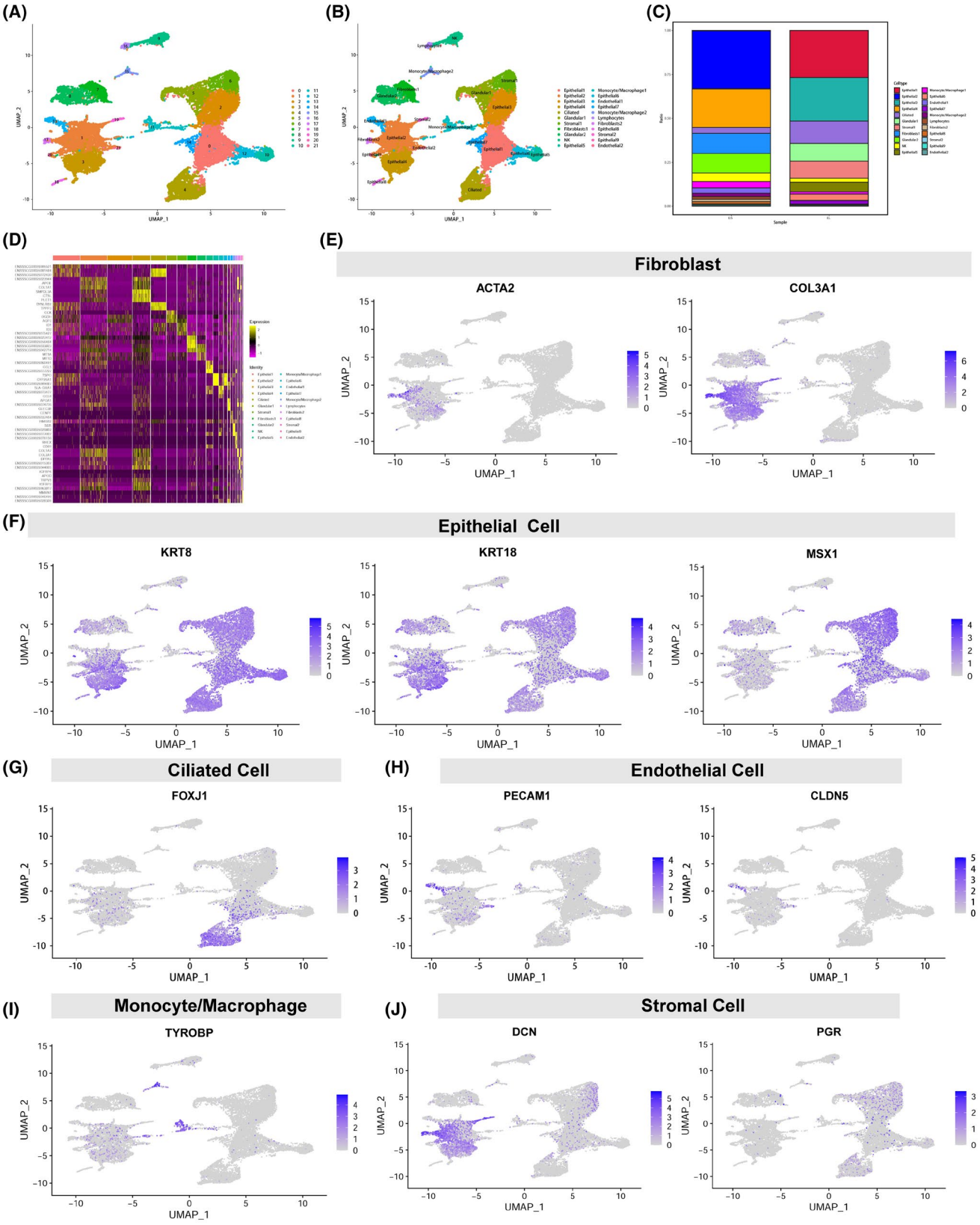

FIGURE 1 Transcription profiles of endometrial cells. (A) UMAP plot of visualizing all cells displayed with different colors for clusters. (B) Integrated UMAP plot of main cell types identified in tissues. (C) The proportion of each cell types in embryo loss (EL) and successful embryo implantation (EIS) tissues. (D) The heatmap of differentially expressed marker genes among different cell types. (E–J). UMAP plot of representative cell markers respectively annotated in fibroblasts, epithelial cell, ciliated cell, endothelial cell, monocyte/macrophage, and stromal cell.

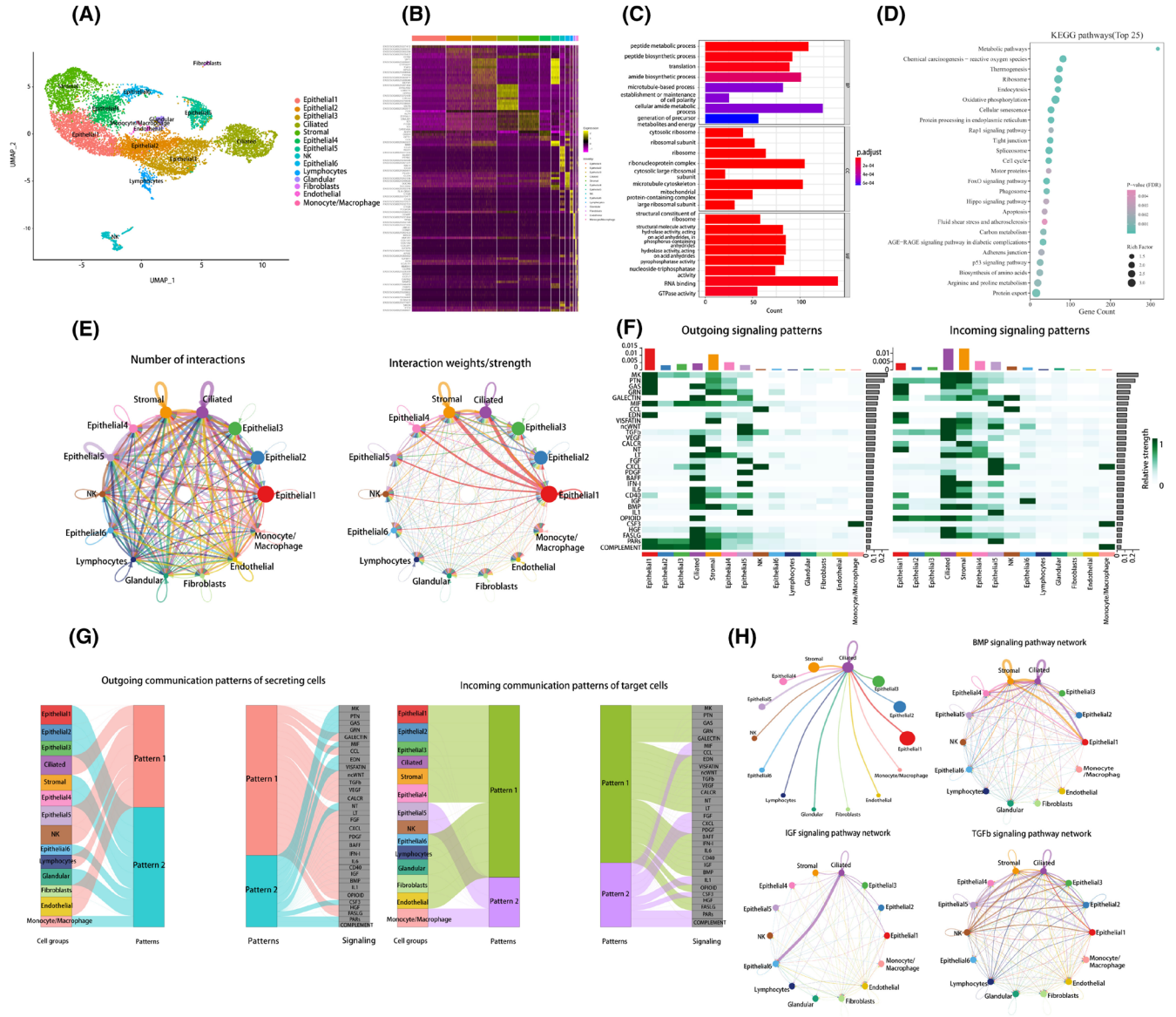

FIGURE 2 Transcription profiles of endometrial cells in EL tissue. (A) UMAP plot of main cell types identified in embryo loss (EL) tissues. (B) The heatmap of differentially expressed marker genes among different cell types in EL tissues. (C) Go functional analysis of EL tissue (p-value <.05). (D) KEGG functional analysis of EL tissue (Top25 pathways, p-value <.05). (E) The chord diagram of the cell communication network in EL tissue (The size of the circle indicates the number of cells, the larger the circle, the greater the number of cells. Cells that emit arrows express ligands, and cells to which the arrows point express receptors, the more ligand-receptor pairs there are, the thicker the line). (F) Potential interactions between subpopulations based on receptor-ligand pairs (p-value <.05). (G) Recognition of intercellular communication patterns in EL tissue. (H) The chord diagram of the cell communication network in ciliated cell, BMP, IGF, and TGF-β signaling pathway network in EL tissue.

that the function of the endometrium in EL tissue was primarily related to the peptide metabolic process, ribonucleoprotein complex, microtubule cytoskeleton, and RNA binding (Figure 2C and Table S5), and the KEGG pathways were mainly enriched in metabolic pathways, reactive oxygen species, and thermogenesis (Figure 2D and Table S6). To further explore the regulation of the endometrial microenvironment by cell-type interactions, we analyzed the expression of ligand-receptor pairs using the Cell Chat software. We noticed that closer receptor-ligand pair dialogs among epithelial cells 1 and other cells had stronger communication strength with ciliated epithelial cells and stromal cells (Figure 2E and Table S7). Ciliated epithelial cells, stromal cells, and epithelial cells 5 were the cell populations that contribute the most to the role of recognizing outgoing or incoming signals, with GRN/VISFATIN/NT/BMP being the strongest contributor to the outgoing signaling of stromal cells, and MK/PTN/CALCR/IFN-1 being the strongest contributor to the incoming signals

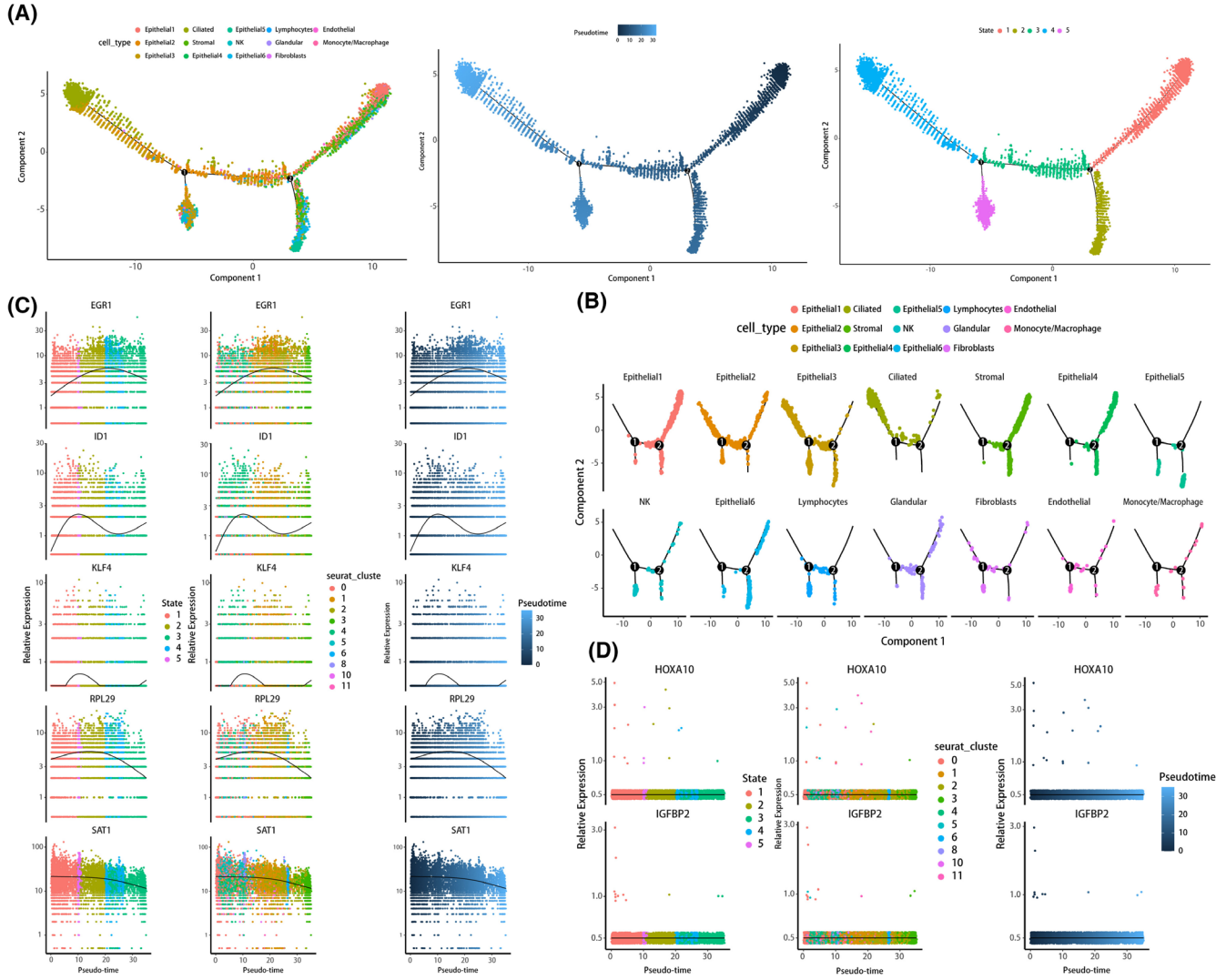

FIGURE 3 Pseudotime trajectory of endometrial cells in embryo loss (EL) tissue. (A, B) Monocle2 analyses showing the development of endometrial cells in EL tissue. (C) Pseudotime trajectory of genes associated with embryo implantation. (D) Pseudotime trajectory of genes associated with endometrial receptivity.

of stromal cells. Additionally, ciliated cells, epithelial cells 5, endothelial cells, NK cells, and lymphocytes have the same pattern, and these patterns are due to the fact that these ncWNT/ FGF/ PDGF/ IFN-1/ IL-1 pathways may have similar outputs. The bone morphogenic pathway (BMP) signaling network was stronger in communication strength among ciliated cells, stromal cells, and epithelial cells 1, while the insulin-like growth factor (IGF) signaling pathway network was stronger in the communication strength of ciliated cells and epithelial cells 6, and the transforming growth factor-β (TGF-β) signaling pathway was stronger between ciliated cells and epithelial cells 5 communication (Figure 2F–H and Table S7). These studies revealed the functional characterization of the endometrium in embryonic loss, with ciliated and stromal cells playing an important role in intercellular communication.

3.3 | Trajectory analysis of endometrial cell in EL tissue

To explore the developmental trajectory of the cell states, we performed a pseudotime analysis of all cell types using monocle2. The developmental trajectory trends of endometrial cells in EL tissues included five stages. Figure 3A shows that stromal cells were at the beginning of differentiation, epithelial cell 1 was at the onset and medium term of differentiation, and ciliated epithelial cells were mainly at the end of differentiation, which may demonstrate the evolution from epithelial cell 1 to epithelial cell 3 and ciliated epithelial cells (Figure 3A,B and Table S8). Based on the important role of epithelial and stromal cells in embryonic attachment, and as the major cell populations in endometrial cells, we further evaluated the temporal expression levels of genes associated with embryo

attachment and endometrial receptivity. Monocle2 analysis showed that genes associated with endometrial receptivity, *HOXA10* and *IGFBP2*, are expressed conservatively in epithelial and stromal cells, indicating that the endometrium is not yet sufficiently receptive to the embryo (Figure 3D). The expression levels of genes related to embryo attachment fluctuated greatly with the change in cell differentiation, and the expression levels of RPL29 and EGR1 first increased and then decreased with the change in cell differentiation (Figure 3C). These studies suggest that ciliated cells are at a stage of terminal differentiation and that the endometrium in which the embryo is lost may not be in the receptivity phase.

3.4 | Transcriptional atlas of endometrial cells in EIS tissues

Sixteen cell types were captured in the EIS tissue, with epithelial and stromal cells being the main cell types (Figure 4A and Table S9). In contrast to the transcriptional profile of endometrial cells in EL tissues, we noted high expression levels of *COL1A1, COL3A1*, and *COL1A2* in epithelial cells 1, these endometrial cell subpopulations with high expression of top maker differed from that in EL tissue (Figure 4B). GO functional enrichment analysis of EIS tissues showed that peptide biosynthetic processes, amide biosynthetic processes, ribosomes, and ribonucleoprotein complex structural constituents of ribosomes were the most enriched (Figure 4C and Table S10). Analysis of intercellular communication in EIS samples (Table S11) showed an increased number of interactions between stromal cells, endothelial cells, and other cells, while the strength of interactions among epithelial cells 1, endothelial cells, and NK cells was stronger (Figure 4D). Epithelial cell 2 is the most important cell population for recognizing outgoing or incoming signaling roles, SPP1 is the largest outgoing signal for epithelial cell 1 and the largest incoming signal for epithelial cell 2. The largest outgoing signals from ciliated epithelial cells were GALECTIN, GAS, BAFF, LT, PDGF, and OPIOID, and the largest incoming signals were GAS, PROS, and BAFF (Figure 4E). We noted close communication in the BMP signaling pathway network among fibroblasts, endothelial cells 1, and ciliated cells, whereas the IGF signaling pathway network showed a strong dialog between endothelial cells 1 and epithelial cells 2, and NK cells had a closer communication with epithelial 1, 2, 3 in TGF-β signaling pathway network (Figure 4F). Additionally, we found that epithelial cells 1, 2, 3, and 4, and NK cells had the same outgoing and incoming communication patterns (Figure S3A). These results revealed that the pattern of intercellular communication was different from that of endometrial cells with unsuccessful gestation.

Next, we evaluated the trajectory of endometrial cell development. The development trajectory of endometrial cells in EIS tissue showed five stages in the timeline (from state 1 to state 2 to state 3 to state 4, or from state 1 to state 5). We found that epithelial cells 1 and 2 were in all states; NK cells, monocytes/macrophages, and endothelial cells were mainly in state 1; ciliated cells were mainly in state 5; and epithelial cells 3 were mainly in states 3 and 4 (Figure 4G and Table S12). Pseudo temporal differentiation trajectories of genes associated with embryo attachment in EIS tissues in endometrial cells showed that the *ID1* gene was barely expressed throughout the differentiation process of endometrial cells, the *EGR1* gene was conservatively expressed throughout the process, the expression levels of the *RPL29 and SAT1* genes showed a trend of decreasing expression levels with the change in differentiation status of the cells, while the expression level of *KLF4* showed a trend of increasing expression levels (Figure S3B). The endometrial receptivity-related gene *HOXA10* was barely expressed by endometrial cells in EIS tissues, whereas the expression of *IGFBP2* first increased and then decreased (Figure S3C). In summary, these results demonstrate that the transcriptional patterns of endometrial cells differ between EIS and EL tissues.

3.5 | Differences in the transcriptional profile of endometrial cell-embryo attachment

Given the important role of estrogen and progestin in endometrial cell proliferation and differentiation, early blastocyst attachment, and maintenance of pregnancy,[23,24] we first assessed the expression levels of PGR and ESR1 genes in the endometrial cells of EL and EIS tissues. Interestingly, *PGR* and *ESR1* were highly expressed in the endometrial cells of EL tissues (Figure 5A,F). The endometrial epithelium is the

FIGURE 4 Transcription profiles of endometrial cells in successful embryo implantation (EIS) tissue. (A) UMAP plot of main cell types identified in EIS tissues. (B) The heatmap of differentially expressed marker genes among different cell types in EIS tissues. (C) Go functional analysis of EIS tissue. (D) The chord diagram of cell communication network in EIS tissue. (E) Potential interactions between subpopulations based on receptor-ligand pairs in EIS tissue. (F) The chord diagram of the cell communication network in ciliated cell, BMP, IGF, and TGF-β signaling pathway network in EIS tissue. (G) Pseudotime trajectory of endometrial cells in EIS tissue.

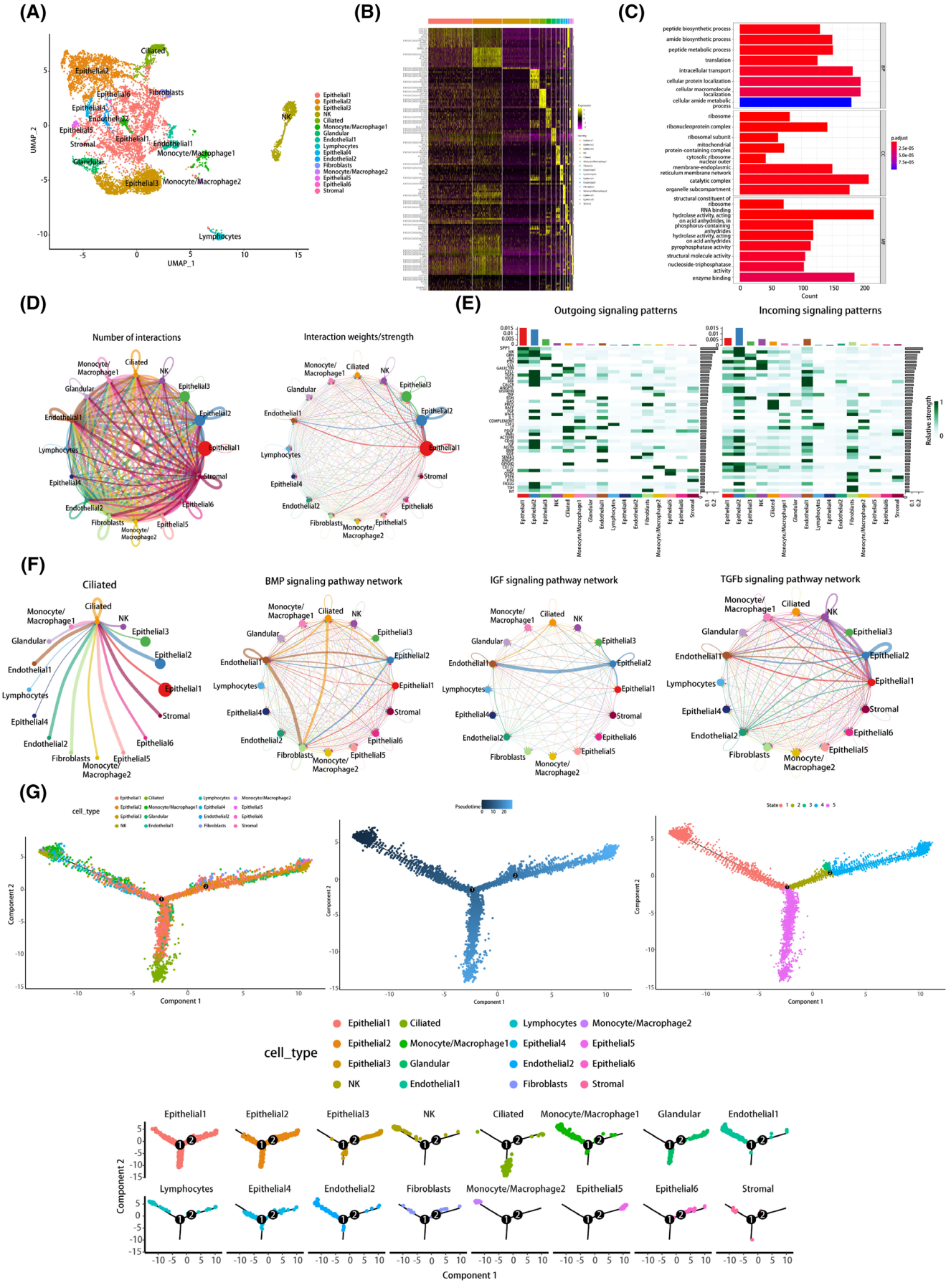
(A)
(B)
(C)
(D)
(E)
(F)
(G)
Ciliated
Epithelial2
Epithelial6
Fibroblasts
Epithelial4
Endothelial2
Epithelial5
Stromal
Epithelial1
Endothelial1
Monocyte/Macrophage1
Glandular
Epithelial3
Monocyte/Macrophage2
NK
Lymphocytes
UMAP_1
UMAP_2
peptide biosynthetic process
amide biosynthetic process
peptide metabolic process
translation
intracellular transport
cellular protein localization
cellular macromolecule localization
cellular amide metabolic process
ribosome
ribonucleoprotein complex
ribosomal subunit
mitochondrial protein-containing complex
cytosolic ribosome
nuclear outer membrane-endoplasmic reticulum membrane network
catalytic complex
organelle subcompartment
structural constituent of ribosome
RNA binding
hydrolase activity, acting on acid anhydrides, in phosphorus-containing anhydrides
hydrolase activity, acting on acid anhydrides
pyrophosphatase activity
structural molecule activity
nucleoside-triphosphatase activity
enzyme binding
Count
p.adjust
Number of interactions
Interaction weights/strength
Outgoing signaling patterns
Incoming signaling patterns
Relative strength
BMP signaling pathway network
IGF signaling pathway network
TGFb signaling pathway network
cell_type
Component 1
Component 2
Pseudotime
State

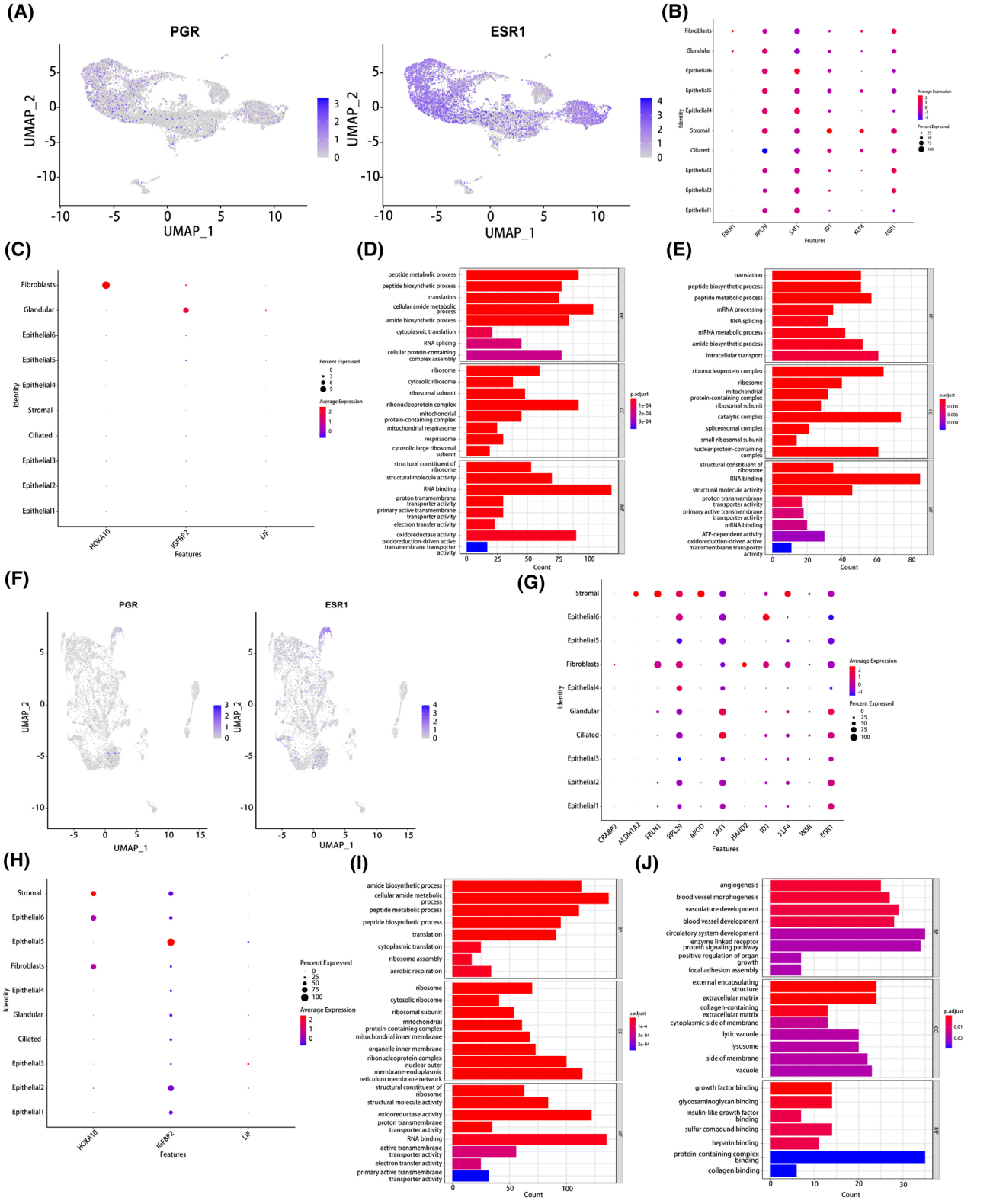

FIGURE 5 Transcriptional characterization of epithelial and stromal cells. (A) UMAP plot of PGR and ESR1 gene in embryo loss (EL) tissue. (B) Bubble map of expression levels of genes associated with embryo attachment in EL tissue. (C) Bubble map of expression levels of genes associated with endometrial receptivity in EL tissue. (D) GO functional analysis of epithelial cells in EL tissue. (E) GO functional analysis of stromal cells in EL tissue. (F) UMAP plot of PGR and ESR1 gene in successful embryo implantation (EIS) tissue. (G) Bubble map of expression levels of genes associated with embryo attachment in EIS tissue. (H) Bubble map of expression levels of genes associated with endometrial receptivity in EIS tissue. (I) GO functional analysis of epithelial cells in EIS tissue. (J) GO functional analysis of stromal cells in EIS tissue.

maternal tissue that establishes close contact with the blastocyst during embryo implantation.[25] Next, we analyzed the expression levels of genes associated with embryo implantation (*CRABP2, ALDH1A2, CST3, FBLN1, RPL29, APOD, SAT1, HAND2, RHOB, ID1, JUN, KLF4, INSR, EGR1, APOLD1, THSD7A*) and endometrial receptivity (*HOXA10, IGFBP2, LIF*) in epithelial and stromal cells. Embryo implantation-related genes (*FBLN1, RPL29, SAT1, ID1, KLF4*, and *EGR1*) were expressed in the EL tissues (Figure 5B), whereas *CRABP2, ALDH1A2, FBLN1, RPL29, APOD, SAT1, HAND2, ID1, KLF4, INSR*, and *EGR1* were expressed in the EIS tissues (Figure 5G). Analysis of genes associated with endometrial receptivity showed that *HOXA10* was expressed in fibroblasts and that *IGFBP2* was expressed mainly in the glandular epithelial cells of EL tissues (Figure 5C). In EIS tissues, *HOXA10* and *IGFBP2* were expressed in the stromal and epithelial cells 5 (Figure 5H). To gain more insight into the differences in epithelial and stromal cell functions in EL and EIS tissues, GO functional enrichment analysis was performed, which revealed that the epithelial cells of EL tissues highly expressed genes involved in peptide metabolic processes, structural constituents of ribosomes, and ribosomes, similar to the function of the epithelial cells of EIS tissues (Figure 5D,I and Tables S13, S14). The analysis of stromal cells of EL tissue was mainly related to translation, ribonucleoprotein complex, and structural constituents of ribosomes, whereas the function of stromal cells in EIS tissue was related to external encapsulating structure, angiogenesis, and growth factor binding (Figure 5E,J and Tables S15, S16). These data indicate that the differences in the transcriptional characteristics of endometrial cell-embryo attachment between EL and EIS were mainly manifested in the epithelial and stromal cells.

3.6 | The heterogeneity of the immune microenvironment of the endometrial cells

It is widely accepted that the immune system plays an important role in embryo-maternal crosstalk.[26] Therefore, we focused on the transcriptional characteristics of immune cells. The immune microenvironment in EL tissues was mainly composed of lymphocytes and NK cells (Figure 6A), whereas that in EIS tissues was dominated by NK cells and monocytes/macrophages (Figure 6G). KEGG functional analysis showed that pathways related to chemokine signaling were most significantly enriched in lymphocytes and monocytes/macrophages of EL tissues (Figure 6B,C), whereas pathways of osteoclast differentiation and lysosomes were dramatically enriched in lymphocytes and monocytes/macrophages of EIS tissues, respectively (Figure 6H,I). The most significantly enriched pathway for NK cells in both tissue types was associated with the ribosomes (Figure 6D,J).

Next, we examined the gene expression profiles of pro- and anti-inflammatory cytokines in EL and EIS tissues. In EL tissues, monocyte/macrophages predominantly expressed the pro-inflammatory cytokine IL-1α, lymphocytes expressed IL-1β, and IL18, NK cells and lymphocytes highly expressed the anti-inflammatory cytokine TGF-β1, and endothelial cells expressed TGF-β2 (Figure 6E,F). In EIS tissues, monocyte/macrophages mainly expressed the pro-inflammatory cytokine IL-1α and IL-1β, lymphocytes expressed IL18, and epithelial cells 5 primarily expressed the anti-inflammatory cytokine IL-6 and TGF-β3, immune cells primarily expressed TGF-β1 (Figure 6K,L). Transcriptional analysis of the immune microenvironment between EL and EIS tissues revealed the heterogeneity of lymphocytes and monocytes/macrophages, and the differences in the pro- and anti-inflammatory microenvironments, suggesting the heterogeneity of immune cells in EL and EIS tissues.

4 | DISCUSSION

Different types of epithelial cells function differently in the development of the endometrium. The luminal epithelium is in direct contact with the conceptus, but the uterine glands contribute to the success of fertility and pregnancy through their secretions, which ensures conceptus survival, implantation, and gestational formation.[27] We identified 12 epithelial cell subpopulations. Epithelial cell 2 and epithelial cell 4 with oxidative phosphorylation functions were abundant in the endometrium at 30 days of gestation, which may be related to the increased energy demand during pregnancy.[28] Ciliated cells transport secretory substances secreted by glands and tubular cells in the uterus,[29] and our work indicates that the number of ciliated cells increased in EL tissue, while previous studies have shown that characteristics of conditions associated with excessive estrogen activity lead to an increased number of ciliated cells.[30] Despite differences in the differentiation trajectories of endometrial cells in EL and EIS tissues, ciliated cells in both tissues were at the terminal end of differentiation, suggesting a high degree of ciliated cell differentiation.[31] Additionally, we found that ciliated epithelial cells were the main output cell population of the IGF signaling pathway in EL tissue, while epithelial cells 2 in EIS tissues are the largest output cell population of the IGF pathway. The IGF-1 in porcine endometrium is associated with embryonic development,[32] promotes the proliferation of uterine epithelial cells in nonpregnant mice.[33] The uterus promotes

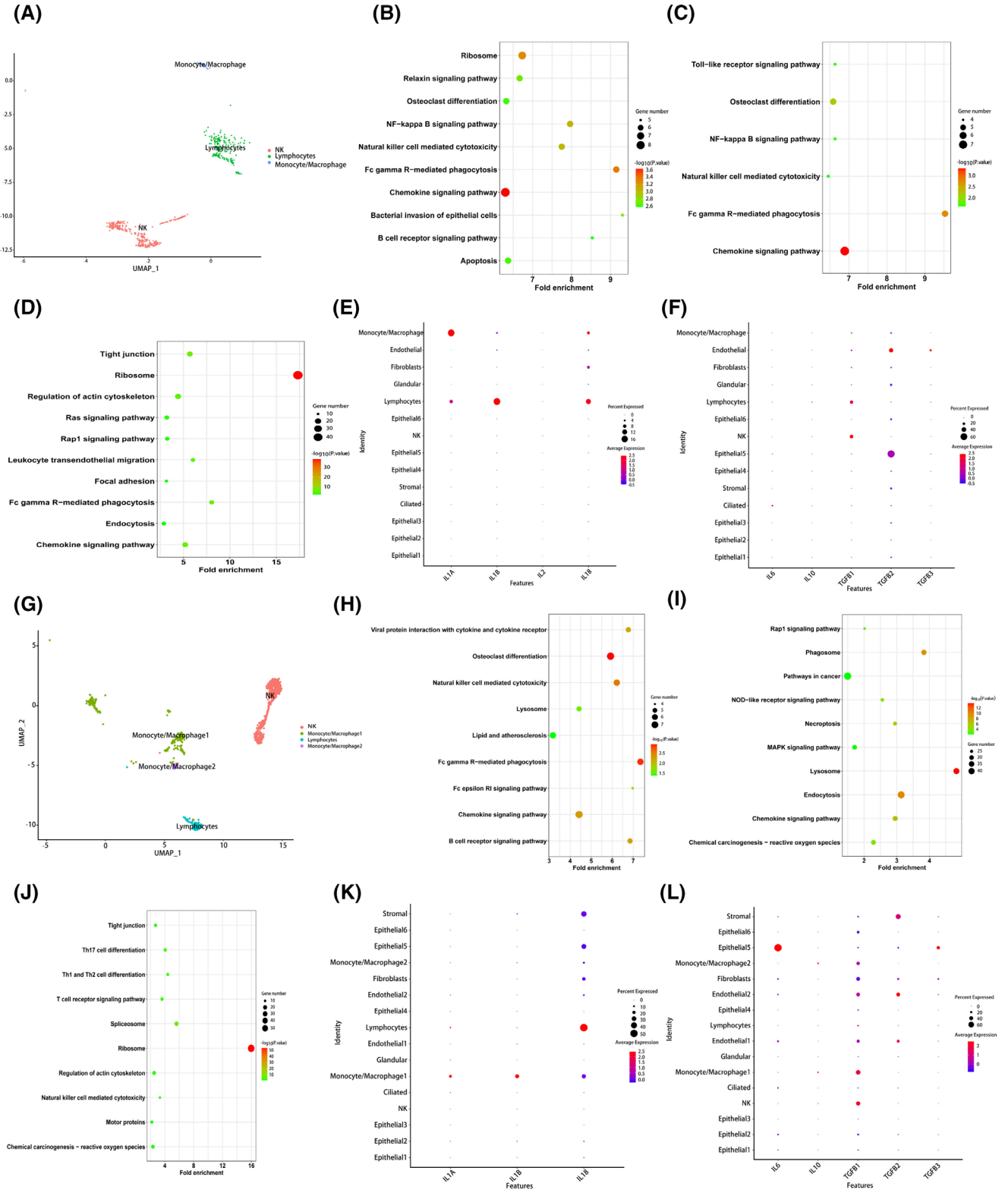

FIGURE 6 The molecular characterization of immune cells. (A) UMAP plot of immune cells in embryo loss (EL) tissue. (B) Kyoto Encyclopedia of Genes and Genomes (KEGG) pathway enrichment analysis of lymphocytes in EL tissue. (C) KEGG pathway enrichment analysis of monocytes/macrophages in EL tissue. (D) KEGG pathway enrichment analysis of NK cells in EL tissue. (E) The bubble map of pro-inflammatory cytokine in EL tissue. (F) The bubble map of anti-inflammatory cytokine in EL tissue. (G) UMAP plot of immune cells in successful embryo implantation (EIS) tissue. (H) KEGG pathway enrichment analysis of lymphocytes in EIS tissue. (I) KEGG pathway enrichment analysis of monocytes/macrophages in EIS tissue. (J) KEGG pathway enrichment analysis of natural killer (NK) cells in EIS tissue. (K) The bubble map of pro-inflammatory cytokine in EIS tissue. (L) The bubble map of anti-inflammatory cytokine in EIS tissue.

early embryonic development and reduces apoptosis, whereas IGFBP3 is present at the maternal-fetal interface and plays a role in implantation and trophectodermal infiltration, associates with the pig litter size trait.[34–36] The regulation of the IGF signaling network in different cell populations in the EL and EIS tissues may be related to endometrial adaptation to the process of embryonic development. On the other hand, complex interactions of the TGF-β signaling pathway network in endometrial cells revealed by analyzing ligand-receptor pair expression in EL tissue, TGF-β is abundantly expressed in the endometrium and secreted into the uterine fluid by endometrial cells and macrophages, possibly interacting with the embryo, enhance pig trophoblast attachment to the endometrium, and the current study found that stromal and glandular cells express TGF-β1 and TGF-β3.[37,38] Bone morphogenic protein is a subgroup of the TGF-β ligand family that mediates transformation of the maternal endometrial microenvironment to support embryo implantation during early pregnancy, and BMPR1B has been identified as a candidate gene for porcine reproductive traits.[39,40] In this study, BMP signaling networks in EIS tissues were significantly enriched in endothelial cells and fibroblasts, while in EL tissues, stromal cells, ciliated cells and epithelial cells 1 were enriched. It has been shown that BMP signaling mutant embryos are able to develop to the post-implantation stage.[41] However, they develop abnormally and die around 8.5 days of embryonic development, and it was concluded that BMP signaling mutations may be the cause of embryo loss.[41] Similarly, SPP1 was found to be the most abundant signal exported and received between epithelial cells 1 and 2, SPP1 is produced by luminal epithelial cells and acts in a paracrine and autocrine manner on trophoblasts and epithelial cells, respectively, to promote normal communication.[42] The above studies suggest that aberrant communication interactions of certain signaling pathways between cells may be the cause of embryo loss or attachment failure.

Because the cause of embryo loss during the peri-implantation period is unclear, we attempted to assess endometrial receptivity and perform molecular characterization of embryo implantation to reveal the cause of embryo loss. Endometrial receptivity is the determining condition for the uterus to provide development of the embryo and adhesion and union of the embryo to the endometrial epithelium, regulated by reproductive hormones.[43] In pigs, the expression of ESR1 and PGR changes with the estrous cycle and pregnancy.[44] We found higher ESR1 and PGR expression levels in EL tissues in this study, and previous studies showed that down-regulation of estrogen receptor-alpha appears to be a critical event that underlies receptivity and that excess estrogenic activity can prematurely close the window for implantation.[45,46]

Next, we revealed endometrial receptivity-related gene expression silencing in EL tissues (*HOXA10, IGFBP2, LIF*, and *PRL*), whereas the *IGFBP2* gene is expressed in EIS tissues and the expression level changes with cell differentiation status. Previous studies have shown that porcine endometrial IGFBP-2 mRNA abundance exhibited stage of pregnancy-dependent induction, the IGFBP-2 gene exhibited abundant mRNA expression in the porcine endometrium at mid/late-pregnancy.[47] Moreover, genes associated with embryo implantation were more abundantly expressed in EIS tissues. We observed that *APOD* genes are mainly expressed in stromal cells in EIS tissues, APOD functions as a multifunctional transporter protein involved in intercellular ligand transport, and the up-regulation of *APOD* in the secreting endometrium is a potential factor in maternal-fetal communication, and *APOD* has been found to be significantly up-regulated in the oviducts and ovaries of guinea pigs during pregnancy.[48,49] The above studies suggest that endometrial hormone level disorders and dysregulated expression of molecular signatures associated with embryo attachment may be responsible for embryo loss.

We observed differences in immune cell function between EL and EIS tissues. NK cells play a role in antigen delivery, autoimmunity, inflammation, and pregnancy; the recognition of target cells by NK cells involves the participation of adhesion molecules and the production of a variety of cytokines such as TNFα, IL-10, IL-1β, and TGFβ.[50,51] Our study found that NK cells in both tissues predominantly expressed the anti-inflammatory cytokine TGF-β1, and the function of NK cells in EL tissues was mainly related to cell adhesion and cell junction-related functions, whereas in EIS tissues it was related to Th cells, and previous studies have shown that the establishment of porcine epitheliochorial placenta is associated with endometrial Th cells recruitment.[52] We also noted an increase in the number of lymphocytes in EL tissues, and it has been found that endometrial NK and variability in T and B lymphocyte populations have all been implicated as contributing factors in adverse reproductive failure outcomes.[53] The embryo secretes growth factors and a variety of inflammatory mediators in addition to estrogen during the peri-implantation process,[54] with days 12–30 of gestation being the critical period during which vascular changes and biogenesis at the maternal–embryonic interface provide nutrients for gestational development. Studies have shown that immune-promoted disruptions in endometrial vasculogenesis are some of the main reasons for the subsequent loss of porcine fetuses and reduction in litter sizes.[15,55,56] Our analysis of the results of inflammatory cytokines secreted by endometrial cells

showed that immune cells in EL tissues mainly expressed inflammatory factors, whereas in EIS tissues, in addition to the release of anti-inflammatory factors by immune cells, anti-inflammatory cytokines were mainly expressed in epithelial and stromal cells, which may be related to the changes in the maternal immune environment in order to achieve a balanced immune status of the body in order to adapt to the immune environment of the fetus during the development process.

In summary, we generated a single-cell transcriptional profile of porcine endometrial cells, including 22 major cell populations, of which epithelial cells, stromal cells, and fibroblasts were the major populations. We determined the ratio of EL and EIS tissue cell populations and characterized the functional characteristics of the major differential cell populations. We found that ciliated epithelial cells had a closer dialog with stromal cells and showed abnormal intercellular communication in the EL tissue. Similarly, we found heterogeneity in the transcription characteristics of embryo implantation-related functions and immune cell functions among endometrial cells of EL and EIS tissues, which provides a referential perspective for research on the endometrium with embryo loss. However, there are some limitations in our study, the cell trajectories are usually determined by the current state of the cell, defined by its gene expression profile, and gene expression itself may not fully reflect the state of the cell.[57] Moreover, the number of samples used in the study was $n=1$ for each group—EL and EIS, and a limited sensitivity to detect low abundance RNAs and technical noise due to the low amount of input material. These limitations contribute to scRNA-seq data having a higher degree of noise compared to bulk RNA-seq data.

AUTHOR CONTRIBUTIONS

Guoliang Zhang, project administration, writing—review and editing, funding acquisition; Tingting Chu, writing—original draft preparation, investigation, and validation; Yadan Jin, formal analysis, methodology, and data curation; Guofang Wu, supervision, resources; Jinyi Liu, resources; Shiduo Sun, validation, and visualization; Yuxuan Song, investigation and project administration. All authors have read and agreed to the published version of the manuscript.

ACKNOWLEDGMENTS

This research was funded by Shaanxi Pig Industry Technology System Breeding and Promotion Integration Project (K3031222128), National Natural Science Foundation of China (31902158), Key Technology R&D Program of Shandong Province (2021LZGC001), Shandong Modern Agricultural Industry Technology System (SDAIT-08-16), Shandong Provincial Natural Science Foundation (ZR2020QC099), Qingdao Natural Science Foundation (24-4-4-zrjj-144-jch), and Research Foundation for Advanced Talents of Qingdao Agricultural University (665/1119013), and we thank Figdraw (https://www.figdraw.com/) that is used to create the graphical abstract.

DISCLOSURES

We declare that none of the authors have any conflict of interest to declare.

DATA AVAILABILITY STATEMENT

The single-cell RNA-seq data are available at the NCBI's Gene Expression Omnibus (GEO) (http://www.ncbi.nlm.nih.gov/gen/) data repository with the accession ID: GSE 282906.

ORCID

Tingting Chu https://orcid.org/0009-0005-3489-8327
Yadan Jin https://orcid.org/0009-0006-6580-0107
Guofang Wu https://orcid.org/0000-0002-5040-1668
Jinyi Liu https://orcid.org/0009-0005-3925-6470
Shiduo Sun https://orcid.org/0000-0002-2714-4173
Yuxuan Song https://orcid.org/0000-0002-5302-7835
Guoliang Zhang https://orcid.org/0000-0003-3253-6638

REFERENCES

1. Cordoba S, Balcells I, Castello A, et al. Endometrial gene expression profile of pregnant sows with extreme phenotypes for reproductive efficiency. *Sci Rep*. 2015;5:14416.
2. Yang Y, Gan M, Yang X, et al. Estimation of genetic parameters of pig reproductive traits. *Front Vet Sci*. 2023;10:1172287.
3. Geisert RD, Ashley EM, Pfeiffer CA, Destiny NJ, Prather RS, Thomas ES. Early embryonic loss is an important mechanism for maximizing litter size in the pig. *J Anim Sci*. 2020;98(4):123.
4. Zang X, Gu S, Wang W, et al. Dynamic intrauterine crosstalk promotes porcine embryo implantation during early pregnancy. *Sci China Life Sci*. 2024;67(8):1676-1696.
5. Wilcox AJ, Weinberg CR, O'Connor JF, et al. Incidence of early loss of pregnancy. *N Engl J Med*. 1988;319(4):189-194.
6. Tian Q, He JP, Zhu C, Zhu QY, Li YG, Liu JL. Revisiting the transcriptome landscape of pig embryo implantation site at single-cell resolution. *Front Cell Dev Biol*. 2022;10:796358.
7. Martinez EA, Angel MA, Cuello C, et al. Successful non-surgical deep uterine transfer of porcine morulae after 24 hour culture in a chemically defined medium. *PLoS One*. 2014;9(8):e104696.
8. Diedrich K, Fauser BC, Devroey P, Griesinger G, Evian Annual Reproduction (EVAR) Workshop Group. The role of the endometrium and embryo in human implantation. *Hum Reprod Update*. 2007;13(4):365-377.
9. Wang Y, Hu T, Wu L, Liu X, Xue S, Lei M. Identification of non-coding and coding RNAs in porcine endometrium. *Genomics*. 2017;109(1):43-50.

10. Geisert RD, Lucy MC, Whyte JJ, Ross JW, Mathew DJ. Cytokines from the pig conceptus: roles in conceptus development in pigs. *J Anim Sci Biotechnol*. 2014;5(1):51.
11. Teh WT, McBain J, Rogers P. What is the contribution of embryo-endometrial asynchrony to implantation failure? *J Assist Reprod Genet*. 2016;33(11):1419-1430.
12. Bui BN, Kukushkina V, Meltsov A, et al. The endometrial transcriptome of infertile women with and without implantation failure. *Acta Obstet Gynecol Scand*. 2024;103(7):1348-1365.
13. Zeng S, Bick J, Ulbrich SE, Bauersachs S. Cell type-specific analysis of transcriptome changes in the porcine endometrium on Day 12 of pregnancy. *BMC Genomics*. 2018;19(1):459.
14. Lessey BA, Young SL. What exactly is endometrial receptivity? *Fertil Steril*. 2019;111(4):611-617.
15. Parrilla I, Gil MA, Cuello C, et al. Immunological uterine response to pig embryos before and during implantation. *Reprod Domest Anim*. 2022;57(Suppl 5):4-13.
16. Bidarimath M, Tayade C. Pregnancy and spontaneous fetal loss: a pig perspective. *Mol Reprod Dev*. 2017;84(9):856-869.
17. Huang J, Yang Y, Tian M, Deng D, Yu M. Spatial transcriptomic and miRNA analyses revealed genes involved in the mesometrial-biased implantation in pigs. *Genes (Basel)*. 2019;10(10):808.
18. Lin J, Liu L, Zheng F, et al. Exploration the global single-cell ecological landscape of adenomyosis-related cell clusters by single-cell RNA sequencing. *Front Genet*. 2022;13:1020757.
19. Lun ATL, Riesenfeld S, Andrews T, et al. EmptyDrops: distinguishing cells from empty droplets in droplet-based single-cell RNA sequencing data. *Genome Biol*. 2019;20(1):63.
20. Butler A, Hoffman P, Smibert P, Papalexi E, Satija R. Integrating single-cell transcriptomic data across different conditions, technologies, and species. *Nat Biotechnol*. 2018;36(5):411-420.
21. Jiang L, Cao D, Yeung WSB, Lee KF. Single-cell RNA-sequencing reveals interactions between endometrial stromal cells, epithelial cells, and lymphocytes during mouse embryo implantation. *Int J Mol Sci*. 2022;24(1):213.
22. Dang D, Taheri S, Das S, Ghosh P, Prince LS, Sahoo D. Computational approach to identifying universal macrophage biomarkers. *Front Physiol*. 2020;11:275.
23. Kim HR, Kim YS, Yoon JA, et al. Estrogen induces EGR1 to fine-tune its actions on uterine epithelium by controlling PR signaling for successful embryo implantation. *FASEB J*. 2018;32(3):1184-1195.
24. Ozturk S, Demir R. Particular functions of estrogen and progesterone in establishment of uterine receptivity and embryo implantation. *Histol Histopathol*. 2010;25(9):1215-1228.
25. Wang HQ, Liu Y, Li D, et al. Maternal and embryonic signals cause functional differentiation of luminal epithelial cells and receptivity establishment. *Dev Cell*. 2023;58(21):2376-2392.e6.
26. Fujiwara H, Ono M, Sato Y, et al. Promoting roles of embryonic signals in embryo implantation and placentation in cooperation with endocrine and immune systems. *Int J Mol Sci*. 2020;21(5):1885.
27. Schmidhauser M, Ulbrich SE, Schoen J. Luminal and glandular epithelial cells from the porcine endometrium maintain cell type-specific marker gene expression in air-liquid interface culture. *Stem Cell Rev Rep*. 2022;18(8):2928-2938.
28. Muccini AM, Tran NT, de Guingand DL, et al. Creatine metabolism in female reproduction, pregnancy and newborn health. *Nutrients*. 2021;13(2):490.
29. Spassky N, Meunier A. The development and functions of multiciliated epithelia. *Nat Rev Mol Cell Biol*. 2017;18(7):423-436.
30. Masterton IARMaRG. The role of oestrogen in the control of ciliated cells of the human endometrium. *Reproduction*. 1976;47:19-24.
31. Mahjoub MR, Nanjundappa R, Harvey MN. Development of a multiciliated cell. *Curr Opin Cell Biol*. 2022;77:102105.
32. Persson E, Sahlin L, Masironi B, Dantzer V, Eriksson H, Rodriguez-Martinez H. Insulin-like growth factor-I in the porcine endometrium and placenta: localization and concentration in relation to steroid influence during early pregnancy. *Anim Reprod Sci*. 1997;46(3–4):261-281.
33. Zhou C, Lv M, Wang P, et al. Sequential activation of uterine epithelial IGF1R by stromal IGF1 and embryonic IGF2 directs normal uterine preparation for embryo implantation. *J Mol Cell Biol*. 2021;13(9):646-661.
34. Green CJ, Span M, Rayhanna MH, Perera M, Day ML. Insulin-like growth factor binding protein 3 increases mouse preimplantation embryo cleavage rate by activation of IGF1R and EGFR independent of IGF1 signalling. *Cells*. 2022;11(23):3762.
35. Herrler A, Einspanier R, Beier HM. Binding of IGF-I to preimplantation rabbit embryos and their coats. *Theriogenology*. 1997;47(8):1595-1607.
36. An SM, Hwang JH, Kwon S, et al. Effect of single nucleotide polymorphisms in IGFBP2 and IGFBP3 genes on litter size traits in Berkshire pigs. *Anim Biotechnol*. 2017;29(4):301-308.
37. Wu YP, Wang AG, Li N, Fu JL, Zhao XB. Association with TGF-β1 gene polymorphisms and reproductive performance of large white pig. *Reprod Domest Anim*. 2010;45(6):1028-1032.
38. Omwandho CO, Konrad L, Halis G, Oehmke F, Tinneberg HR. Role of TGF-betas in normal human endometrium and endometriosis. *Hum Reprod*. 2010;25(1):101-109.
39. Liao Z, Tang S, Jiang P, et al. Impaired bone morphogenetic protein (BMP) signaling pathways disrupt decidualization in endometriosis. *Commun Biol*. 2024;7(1):227.
40. Liu Z, Xu R, Zhang H, Wang D, Wang J, Wu K. A unique 15-bp InDel in the first intron of BMPR1B regulates its expression in Taihu pigs. *BMC Genomics*. 2022;23(1):799.
41. Sozen B, Demir N, Zernicka-Goetz M. BMP signalling is required for extra-embryonic ectoderm development during pre-to-post-implantation transition of the mouse embryo. *Dev Biol*. 2021;470:84-94.
42. Jane E, Garlow HK, Greg A, et al. Analysis of osteopontin at the maternal-placental interface in pigs. *Biol Reprod*. 2002;66:718-725.
43. Llobat L. Embryo gene expression in pig pregnancy. *Reprod Domest Anim*. 2020;55(4):523-529.
44. Ka H, Seo H, Choi Y, Yoo I, Han J. Endometrial response to conceptus-derived estrogen and interleukin-1β at the time of implantation in pigs. *J Anim Sci Biotechnol*. 2018;9:44.
45. Lee DK, Kurihara I, Jeong JW, et al. Suppression of ERalpha activity by COUP-TFII is essential for successful implantation and decidualization. *Mol Endocrinol*. 2010;24(5):930-940.
46. Ma WG, Song H, Das SK, Paria BC, Dey SK. Estrogen is a critical determinant that specifies the duration of the window of uterine receptivity for implantation. *Proc Natl Acad Sci U S A*. 2002;100(5):2963-2968.
47. Song S, Lee CY, Green ML, Chung CS, Simmen RC, Simmen FA. The unique endometrial expression and genomic

organization of the porcine IGFBP-2 gene. *Mol Cell Endocrinol*. 1996;120(2):193-202.
48. Germeyer A, Capp E, Schlicksupp F, et al. Cell-type specific expression and regulation of apolipoprotein D and E in human endometrium. *Eur J Obstet Gynecol Reprod Biol*. 2013;170(2):487-491.
49. Provost PR, Tremblay Y, El-Amine M, Belanger A. Guinea pig apolipoprotein D RNA diversity, and developmental and gestational modulation of mRNA levels. *Mol Cell Endocrinol*. 1995;109(2):225-236.
50. Sciezynska A, Komorowski M, Soszynska M, Malejczyk J. NK cells as potential targets for immunotherapy in endometriosis. *J Clin Med*. 2019;8(9):1468.
51. Faas MM, de Vos P. Uterine NK cells and macrophages in pregnancy. *Placenta*. 2017;56:44-52.
52. Dimova T, Mihaylova A, Spassova P, Georgieva R. Establishment of the porcine epitheliochorial placenta is associated with endometrial T-Cell recruitment. *Am J Reprod Immunol*. 2007;57(4):250-261.
53. Marron K, Harrity C. Endometrial lymphocyte concentrations in adverse reproductive outcome populations. *J Assist Reprod Genet*. 2019;36(5):837-846.
54. Mathew DJ, Lucy MC, Geisert RD. Interleukins, interferons, and establishment of pregnancy in pigs. *Reproduction*. 2016;151(6):R111-R122.
55. Stenhouse C, Hogg CO, Ashworth CJ. Novel relationships between porcine fetal size, sex, and endometrial angiogenesisdagger. *Biol Reprod*. 2019;101(1):112-125.
56. Nicola F, Linton JMW, Cnossen SA, Croy BA, Tayade C. Immunological mechanisms affecting angiogenesis and their relation to porcine pregnancy success. *Immunol Investig*. 2009;37(5–6):611-629.
57. Tritschler S, Büttner M, Fischer DS, et al. Concepts and limitations for learning developmental trajectories from single cell genomics. *Development*. 2019;146(12):dev170506.

SUPPORTING INFORMATION

Additional supporting information can be found online in the Supporting Information section at the end of this article.

How to cite this article: Chu T, Jin Y, Wu G, et al. Insights into the single-cell transcriptome characteristics of porcine endometrium with embryo loss. *The FASEB Journal*. 2025;39:e70395. doi:10.1096/fj.202402212RR